iScience

CellPress
OPEN ACCESS

Article

A binocular perception deficit characterizes prey pursuit in developing mice

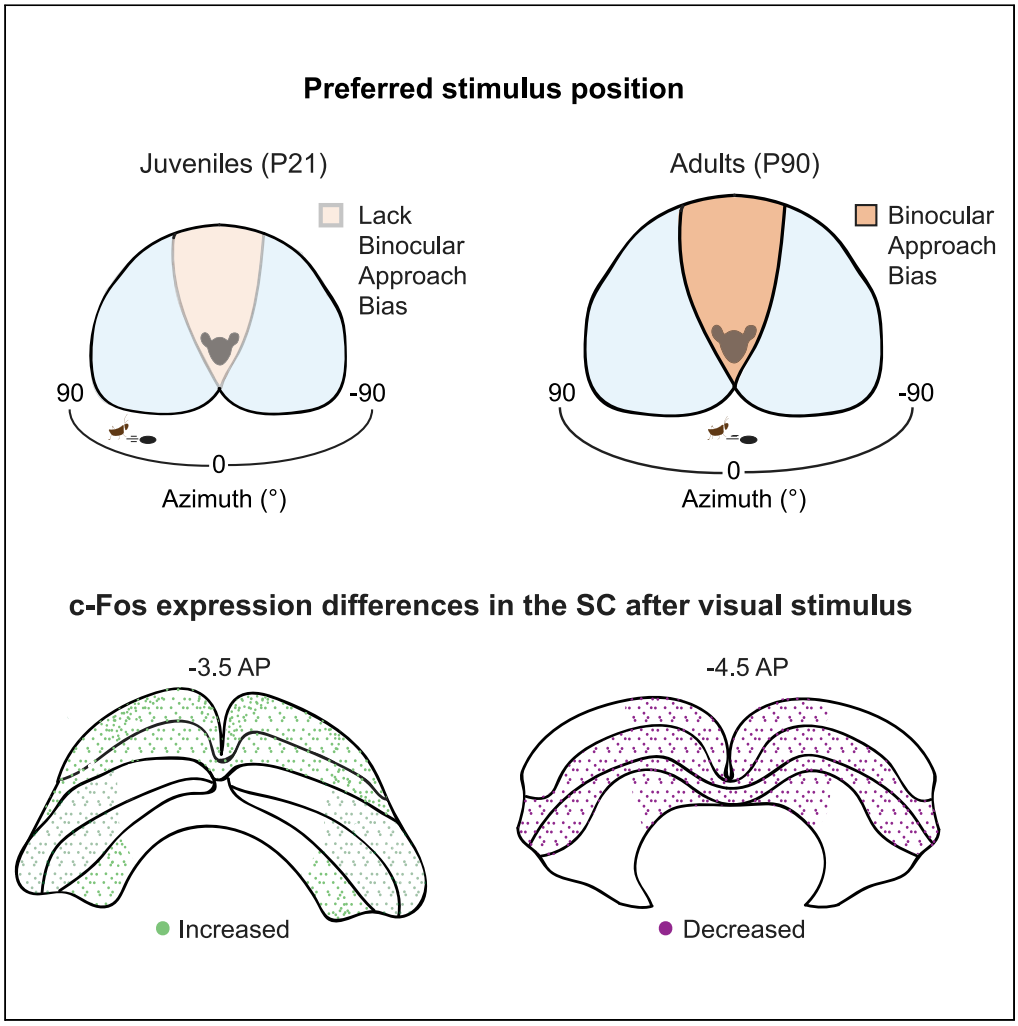

Kelsey Allen, Rocio Gonzalez-Olvera, Milen Kumar, Ting Feng, Simon Pieraut, Jennifer L. Hoy

jhoy@unr.edu

Highlights

Juvenile (P21) mice robustly investigate live insects

Insect pursuit behavior relying on binocular vision is immature in P21 mice

Visually induced arrest responses are similar between P21 and adult mice

c-Fos expression selectively increases in juvenile SC after visual experience

Allen et al., iScience 25, 105368
November 18, 2022
https://doi.org/10.1016/j.isci.2022.105368

iScience

CellPress
OPEN ACCESS

Article

A binocular perception deficit characterizes prey pursuit in developing mice

Kelsey Allen,[1] Rocio Gonzalez-Olvera,[1] Milen Kumar,[1] Ting Feng,[1] Simon Pieraut,[1] and Jennifer L. Hoy[1,2,*]

SUMMARY

Integration of binocular information at the cellular level has long been studied in the mouse model to uncover the fundamental developmental mechanisms underlying mammalian vision. However, we lack an understanding of the corresponding ontogeny of visual behavior in mice that relies on binocular integration. To address this major outstanding question, we quantified the natural visually guided behavior of postnatal day 21 (P21) and adult mice using a live prey capture assay and a computerized-spontaneous perception of objects task (C-SPOT). We found a robust and specific binocular visual field processing deficit in P21 mice as compared to adults that corresponded to a selective increase in c-Fos expression in the anterior superior colliculus (SC) of the juveniles after C-SPOT. These data link a specific binocular perception deficit in developing mice to activity changes in the SC.

INTRODUCTION

Our understanding of the development of visual circuit function is significantly advanced by employing the mouse model (see[1–4] for representative reviews). For example, we know when neurons in the primary visual cortex acquire their ability to integrate binocular input and we know that several important mechanisms required for this development are conserved across species.[1,4–6] However, we do not yet understand how to relate these developmental differences in cellular function of the cortex to natural visual behavior in developing mice. Nor do we understand whether and when significant developmental changes in other visual areas, such as the superior colliculus (SC), lead to important changes in visual behavior across development. The mouse SC in particular represents a rich repertoire of visual information, including binocularity and stimulus motion, size and valence.[7–10] The SC also controls many important and highly conserved visual behaviors in the adult mouse such as predator/stimulus avoidance and prey capture/stimulus pursuit.[10–14] Thus, to best understand how known mechanisms of visual circuit plasticity relate to visual behavior, it is necessary to better understand these two aspects of mouse visual system development: (1) Age-characteristic binocular behavior and 2) the relationship between binocular behavior and SC circuit maturation.

Studying the development of innate visual behavior will allow us to better establish the causal relationships between the refinement of visual neural circuits and behavior in the mouse.[11,12] In particular, the complex visual processing required for mice, other rodents and primates to capture prey is an ideal natural context to investigate visual system circuit development as related to object identification, visual search and determining stimulus salience and stimulus pursuit.[13–16] Specifically, prey pursuit entails complex visual control over motor movements which requires accurate spatial localization of targets and predictive coding to be successful.[15,17,18] There is also evidence that juvenile mammals and barn owls must have adequate time to practice the behaviors needed for prey capture to survive in the wild.[19,20] In addition, larval zebrafish demonstrate remarkable plasticity in prey capture behavior that requires increasing integration between the tectum (homologous to the SC) and forebrain circuitry.[21] Similarly, adult mice significantly change their responsiveness to virtual "prey-like" stimuli presented in our computerized-spontaneous perception of objects task (C-SPOT) after having previous experience with live crickets.[22] This emerging body of work suggests that studying the development of visually guided prey capture in the mouse as related to SC circuit development will uncover key molecular and cellular mechanisms underlying plasticity of conserved and fundamental aspects of vision.

Binocular integration within the superior colliculus mediates optimal visually guided prey capture in the adult mouse.[23,24] Monocular occlusion[23] or perturbation of ipsilateral retinal input to the SC[24] leads to

[1]Department of Biology, University of Nevada, Reno, Reno, NV 89557, USA

[2]Lead contact

*Correspondence: jhoy@unr.edu

https://doi.org/10.1016/j.isci.2022.105368

an increase in time to capture a live insect and reduces that ability of mice to maintain pursuit of prey within their binocular zone. However, these recent studies did not quantify whether juvenile mice exhibited insect hunting, or hunting-like behavior, nor whether binocular-dependent perceptions and/or prey capture-related activity in the superior colliculus might be developmentally regulated in the mouse. In this study, we compared both live prey capture behavior and innate responses to virtual "prey-like" visual stimuli between P21 and adult mice. Our analyses revealed that P21 mice lack a prominent binocular visual field bias that enhances successful "target" approach and pursuit in the adult during both the live and virtual behavioral assays. C-SPOT in particular revealed that visually guided approach behavior was specifically different in early development relative to visually induced arrest behavior driven most frequently by small moving objects appearing in the monocular visual field. To connect developmental differences in visual pursuit behavior to possible differences in SC activity, we compared c-Fos expression levels in the SC between P21 and adult mice. Analysis of c-Fos[26] expression in the SC after C-SPOT revealed a distinct pattern of enhanced cellular activity in the anterior regions of the SC in juveniles responding to visual motion stimuli relative to adults. Our results indicate cellular activity differences in the anterior SC as relevant to developmental differences in binocular perception and the accurate pursuit of visual objects in mice. Overall this approach may be a useful way to assay sensory processing differences in mouse models of neurodevelopmental disorders that impact visual system plasticity.[27]

RESULTS

To understand how the mouse relates to other species such as the owl where the young practice and improve prey capture behavior,[19] we first determined whether postnatal day 21 (P21) mice, before weaning and foraging for themselves, also use vision to detect, approach and pursue live insects (Figure 1). The house mouse, a popular model of mechanistic visual system development, readily approaches and ultimately preys on live insects using specific visual cues.[13] This behavior relies on specific neural circuitry in the superficial superior colliculus.[25] P21 laboratory mice of several background strains (see STAR methods) also detect, approach and engage live crickets repeatedly in the laboratory setting (Video S1, juvenile live prey capture, associated with data in Figure 1). No significant differences were observed on measures of prey capture performance between the C57BL/6J wild type and mixed background strains used in this study ($p > 0.10$ in all cases, Time to first Approach, Probability of Intercept and Duration of Contact, C57BL/6J versus Ntsr1-GN209-Cre mice and C57BL/6J versus Grp-KH288-Cre mice, Welch's t-test, with correction for multiple comparisons, 3 comparisons). We note several important differences between P21 and adult mice (Video S2, adults live prey capture, associated with data in Figure 1), specifically in approach orienting responses when they first encounter live crickets. Most dramatically, P21 mice fail to show a binocular visual field bias on initiating an approach relative to adults (Figure 1A). This correlates with a significant increase in the onset of the first approach toward a cricket by P21 mice versus adults (Figure 1B). Overall, these differences do not result in a decline in the total number of approaches started over the entire 5-min encounter with a live cricket (16.1 ± 1.2 versus 17.5 ± 2.1, P21 vs. P90, $N = 12$ vs. 10, respectively, $p > 0.05$, Welch's t-test, Videos S1 vs. S2). The detection and pursuit deficits correlate with a significant decrease in the probability that an approach started will end with a successful contact (Figure 1C and Videos S1 vs. S2). Furthermore, when P21 mice successfully contact live crickets, they do so from a wider mean stimulus angle at the end of approach (48.3 ± 2.2 versus 26.1 ± 0.5, P21 versus P90, $N = 12$ versus 10, respectively, $p < 0.01$, Welch's t-test) and engage in prolonged proximate contact with rapid sniffing (Figure 1D). Related to this behavior, juvenile mice rarely attack insects even after repeated exposure over 5 days relative to adults (18.2 versus 80% of juveniles versus adults attacked crickets after 5 days of exposure for 5 min each day, Fisher Exact test, $p = 0.0046$, $N = 11$ versus 10, respectively), both groups without food deprivation. Taken together, these results indicate that the binocular visual field bias that facilitates adult mouse approach and pursuit behavior is immature in P21 mice. This developmental timepoint corresponds to a known inability to integrate binocular information as studied in visual cortex.[1,28,29] However, the behavioral deficit could also relate to possible immaturity of binocular responses located in the mouse superior colliculus.[9,30] Consistent with this idea, induced perturbation of ipsilateral eye input to the superior colliculus in adults results in similar prey capture behavior deficits as we show characterize normally developing juveniles.[24]

Though live prey capture analysis captured a binocular processing deficit in developing mice, it is a complex multimodal experience relying on more sensory input than just vision,[13] especially in insect-naïve mice.[31] We therefore quantified the innate visual behavior of P21 mice evoked by virtual, high-contrast motion stimuli displayed from a computer screen using a computerized, spontaneous perception of

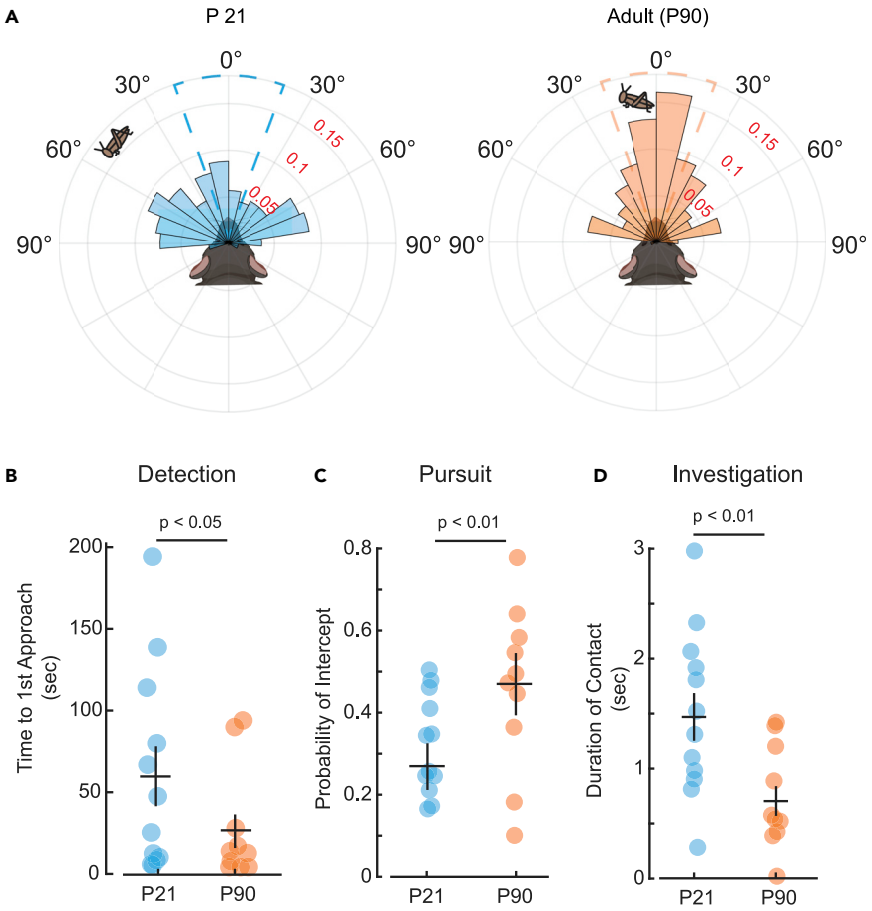

Figure 1. Analysis of natural prey capture behavior reveals a lack of binocular visual field bias to start approaches in P21 mice relative to adults

(A) Normalized polar plot distributions of stimulus angles (angle between mouse bearing and position of cricket) where successful approaches in juveniles (left) versus adults (right) began.

(B) Detection behavior as measured by time to start an approach by P21 mice, blue, versus P90 mice, orange.

(C) Probability of cricket interception, an approach that ends in cricket contact.

(D) Stimulus investigation-related behavior indicated by the duration of a contact. Welch's t-test, N = 11 versus 10, P21 mice versus P90 mice, respectively, Error bars are +/− standard error of the mean.

objects task, C-SPOT.[22] C-SPOT affords the opportunity to vary specific parameters of visual objects and quantify how that alters stimulus detection and response relative to the egocentric location of the objects that cause behavioral responses (Figures 2A–2C). Although mice have not been presented with all possible combinations of "cricket-like" features using C-SPOT, mice that experience cricket capture specifically increase approach responses to a simple moving ellipse of a particular combination of size and speed.[22] We presented this "cricket-like" stimulus to both adults and P21 juveniles (Figure 2A) and found striking developmental differences in orienting behaviors (Figures 2D and 2E). Both ages robustly approach the presented virtual stimulus over a total 5-min presentation period. However, P21 mice take significantly longer to first approach (Figures 2D and 2F) and generate fewer approaches toward the stimulus over the entire session (Figures 2D and 2G). On the other hand, P21 and adult mice arrest their locomotion in response to stimuli with similar latencies from the start of stimulus presentation and have a similar arrest frequency overall (Figures 2D–2F and 2H). This suggests that P21 mice still detect the moving stimuli as rapidly as adults and find motion in their periphery salient. Further, there are no significant sex differences in the measured behaviors (Figures 2G and 2H, $p > 0.05$, Welch's t-test, correction for multiple comparisons, 2 comparisons total), Thus, P21 deficits in visual processing are specific to the relative visual information that elicits an approach and allows stimulus interception. The increase in latency to approach the virtual targets by P21 mice is consistent in both our C-SPOT assay and live prey capture. This argues that a developmental

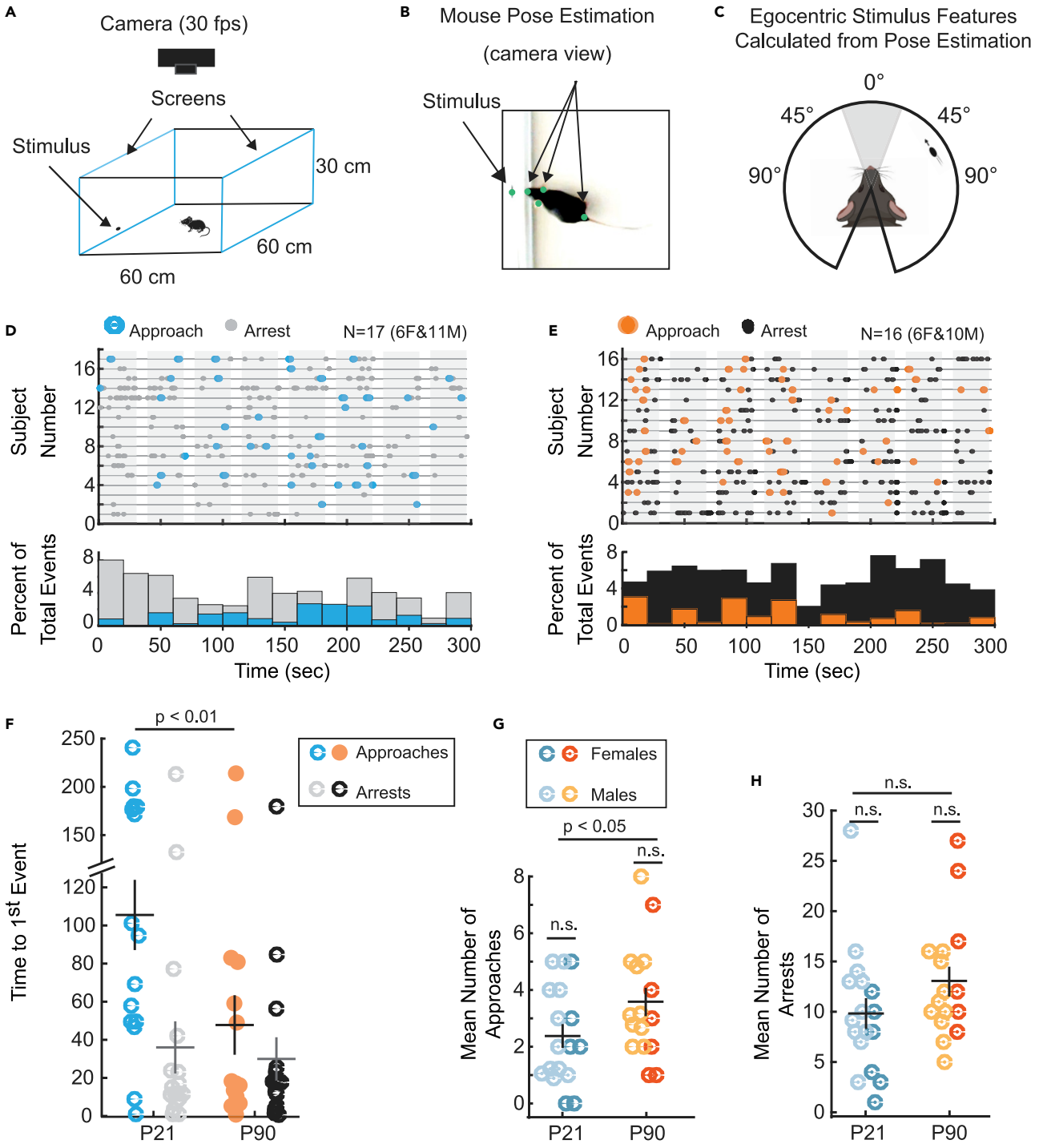

Figure 2. C-SPOT reveals robust developmental differences in innate visual orienting behavior

(A) Left, schematic of experimental arena. Blue outlines indicate location of computer monitors displaying stimuli and illuminating the environment.

(B) Example frame from a recorded behavioral video overlaid with post estimates of relevant points.

(C) Analysis of tracked positions in B, are used to generate estimates of egocentric visual features: relative stimulus size, speed, and position along the azimuth of the visual field (stimulus angle).

(D and E) Ethograms of each subjects' response (subject ID on y axis) over time in seconds revealing when during each stimulus "sweep" (30 s, shaded in gray) approaches (color) or arrests (gray or black) occurred from stimulus onset. Ethograms are aligned to the start of 1st stimulus presentation. Below, histograms showing the proportion of response type, either an approach (blue)or arrest (gray), that occurred during each 20 s bin of time.

Figure 2. *Continued*

(F) Mean time to first orienting event of either approaches (colors) versus arrests (gray and black).

(G) Mean number of approach starts and (H) Mean number of arrests. Significance determined using Welch's t-test, N = 17 versus 16, P21 versus P90 mice, respectively. n.s. = not significant. Error bars are +/− standard error of the mean.

difference in visuo-motor integration specifically explains the developmental differences in live prey capture behavior.

To determine more precisely which visual responses and stimulus preferences are different between P21 mice and adult mice, we quantified the visual field location, relative size (in arc degree), and speed (in arc degree/sec) of the virtual stimulus at the onset of an approach or arrest response (Figure 3). Consistent with what was observed during live prey capture, P21 mice lack a strong binocular visual field bias in first detecting stimuli that they then successfully and continuously approach (Figures 3A and 3B, Left). In contrast to adults, the average position of stimuli that are approached is near 60° (Figure 3C). In addition, when P21 mice nearly contact the stimulus with the nose, they reach a position just in front of the stimulus whereas adults end with their nose touching at or near the center of the stimulus (Videos S3 versus S4, juvenile versus adult responses to virtual stimuli during C-SPOT, associated with data in Figures 3 and 4). This leads to a significant difference in mean absolute stimulus angle at the end of an approach (33.1 $\pm$ 7.2 vs. 11 $\pm$ 4.3, P21 vs. P90, N = 15 vs. 16, respectively, $p < 0.05$, Welch's t-test). Taken together, these data demonstrate that P21 mice similarly detect and respond to stimuli located in their peripheral visual field, but specifically have a deficit in how they respond to stimuli that are located in central-anterior egocentric space, where visual information can be processed binocularly for adult animals.

Importantly, our assay revealed that the perception of stimuli that cause approach are specifically developmentally regulated relative to those perceptions that elicit arrest. For both ages, the stimuli that are likely to elicit arrest responses are primarily located in the periphery, but otherwise do not vary significantly in relative size or speed between juveniles and adults (Figures 3D and 3E). This suggests that the visual pathways that process peripheral, monocular visual information may have similar spatial and temporal resolution capabilities and lead to similar arrest behavioral outcomes at both ages. Indeed, we showed that the arrest responses evoked by these objective stimuli in the adults depend on the egocentric direction of motion of the stimulus across the visual field.[22] That is, stimuli that elicited arrests not followed by an approach were moving further into the peripheral monocular visual field of mice. In addition, both ages of mice were able to detect stimuli that caused either an approach (Figure 3A) or an arrest from the furthest possible reaches of the testing environment, ~60cm from the mouse (Figure 3). Thus, P21 mice are capable of responding to similar relative sizes and speeds of objects as compared to adults. Importantly, we did not probe the capabilities of the juvenile visual system in this study exhaustively. Receptive field properties do refine after eye-opening even in the monocular visual field of primary visual cortex suggesting that other aspects of monocular visual behavior may yet mature over development.[32] Thus, our future studies will seek to parametrically test a wider range of qualities of motion to further probe for differences in visual perception that change over development in a retinotopic fashion.

To map developmental differences in mouse visual orienting behavior to possible differences in activity in the SC, we assayed the expression of the immediate-early gene c-Fos (Figure 4). We reasoned that this topographically organized, evolutionarily conserved, visual area may display significant differences in c-Fos activation as it has been significantly linked to generating representations of stimulus salience, direction of motion, relative size and speed of visual objects (see Basso et al.,[33] for a recent review). Furthermore, specific cell types within the SC are required to control orienting behavior in the adult mouse during prey capture[25] and the deeper layers that are aligned to the superficial retinotopy are known to integrate multimodal sensory input (visual, auditory and somatosensory) relevant to prey capture behavior.[31,34,35] We quantified the percent of c-Fos positive cells in different regions of the SC in mice exposed to C-SPOT versus age-matched controls exposed to the same environment with no stimuli presented (Figure 4). We obtained measures at three different locations along the anterior-posterior axis (−3.5, −4.15 and −4.6 AP) to compare regions of SC that encode visual information along the nasal (central) to temporal (peripheral) visual field axis.[34,35] We also compared across the three laminar zones from the dorsal surface (superficial, intermediate, and deep) and medial versus lateral divisions of the SC at the three positions along the AP axis (Figures 4A and 4B). We calculated a ratio of c-Fos positive cells after visual stimulation normalized to age-matched controls with no stimuli in the same environment in each subregion of the SC. We then statistically compared those ratios between comparable subregions from the two ages of mice using Welch's

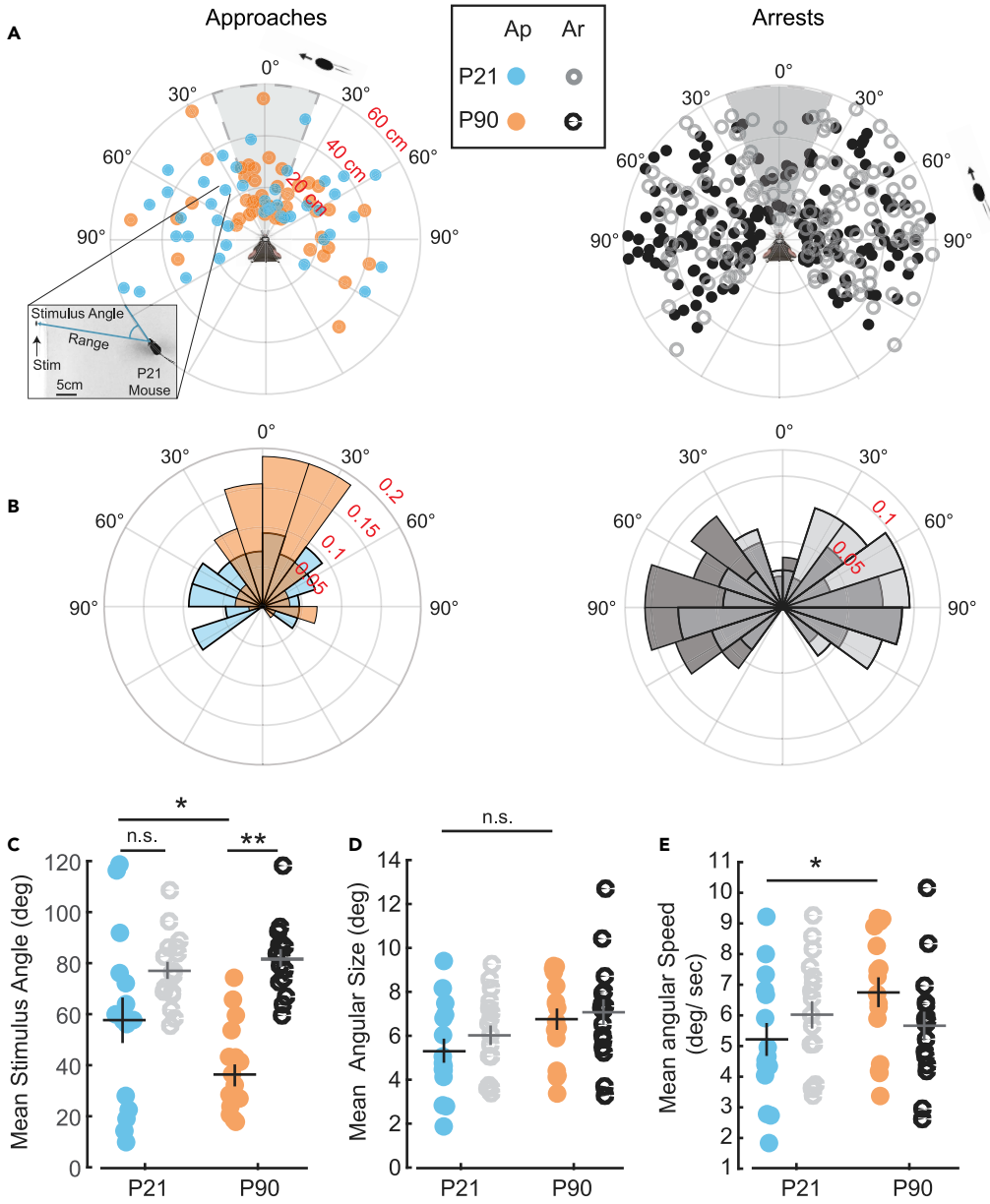

Figure 3. P21 mice show specific binocular visual field deficits at start of approach toward stimulus in the C-SPOT assay

(A) Polar plot distribution of individual approach starts (Left) and arrests (Right) evoked by a virtual visual stimulus for P21 (blue) versus P90 (orange) mice. Plotted is range (cm) versus stimulus angle (degree). Inset shows a frame from a P21 behavior video where an approach started toward a stimulus from a stimulus angle of ~35° from about 22cm away from the screen (represents blue point where call out to inset begins).

(B) Normalized polar plots of approaches (Left) or arrests (Right) by age. Plotted is fraction of total events versus stimulus angle (degree).

(C) Mean stimulus angle for each subject at approach starts (color) or arrests (black and gray).

(D) Mean subjective size of stimulus (visual angle in degrees) when approaches (color) or arrests (black and gray) start.

(E) Mean subjective speed of stimulus (degrees/sec) when approaches or arrests start. Significance determined using Welch's t-test, with Benjamini-Hochberg procedure to correct for multiple comparisons, N = 17 versus 16, P21 versus P90 mice, respectively. n.s. = not significant, * = $p < 0.05$, ** = $p < 0.01$. Error bars are +/− standard error of the mean.

A Sampling c-Fos Expression Relative to Topographical Organization of SC

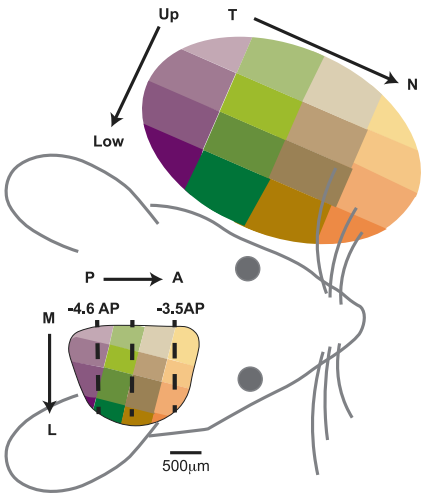

B Ratio c-Fos Expression (w to w/o Visual Stimulation)

		P21		P90	
		Medial	Lateral	Medial	Lateral
-3.5 AP	S	**2.92 ± 0.48**	**2.72 ± 0.39**	1.00 ± 0.17	0.94 ± 0.15
	I	**1.65 ± 0.23**	**2.26 ± 0.34**	1.17 ± 0.26	0.82 ± 0.09
	D	**2.69 ± 0.32**	**2.17 ± 0.29**	1.11 ± 0.16	1.09 ± 0.28
-4.1 AP	S	**1.78 ± 0.22**	**2.38 ± 0.51**	0.58 ± 0.13	0.80 ± 0.16
	I	1.12 ± 0.17	1.83 ± 0.70	0.85 ± 0.12	0.83 ± 0.10
	D	1.64 ± 0.80	2.40 ± 1.60	0.76 ± 0.30	0.74 ± 0.15
-4.6 AP	S	1.38 ± 0.14	1.47 ± 0.49	**0.50 ± 0.14**	0.83 ± 0.11
	I	**0.64 ± 0.12**	**0.85 ± 0.08**	**0.56 ± 0.08**	**0.60 ± 0.07**
	D	0.72 ± 09	1.05 ± 0.17	**0.50 ± 0.13**	0.84 ± 0.17

C

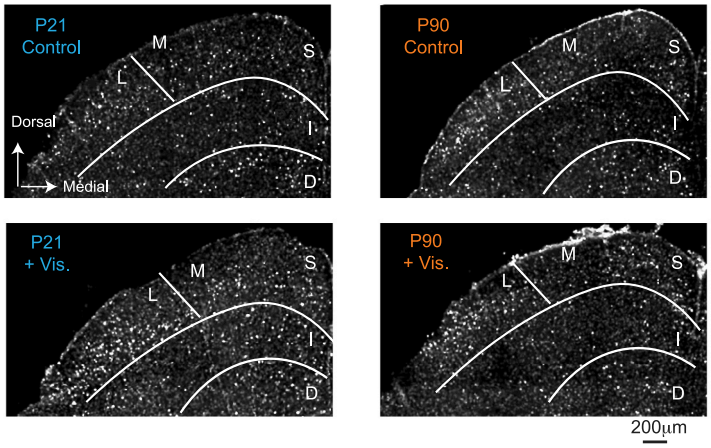

D

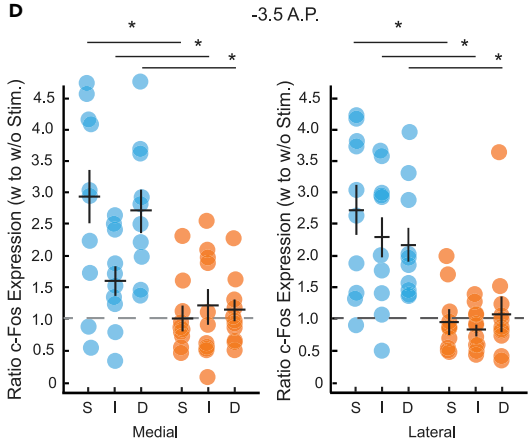

Figure 4. c-Fos expression differences after C-SPOT in P21 versus P90 mice

(A) Adaptation of visual field topography reflected in the right hemisphere of the superior colliculus of the mouse from a dorsal view, Dräger and Hubel, 1976. The cartoon is meant as general representation of visual space in the superficial SC that is observed during topographical imaging of mouse SC.[2] We assayed for c-Fos expression differences after exposure to virtual visual stimuli that evoke approach and arrest behaviors from three key planes of coronal sections, −3.5 anterior-posterior (AP), −4.1 AP and −4.6 AP (black dashed lines spanning the SC). A = anterior, P = posterior, M = medial, L = lateral, T = temporal, N = nasal, Up = upper visual field displayed to the mouse's left eye and Low = lower visual field.

(B) Table summarizing the mean ratio of c-Fos expression (percent of cells positive for c-Fos) in mice exposed to visual stimuli in C-SPOT relative to those w/out visual stimulation in the same environment. Ratios are normalized by dividing each subject's percent of c-Fos positive cells by the mean of the percent of c-Fos positive cells in an age-matched control group, e.g., a ratio of 2.92 means a mouse after C-SPOT had nearly 3 times as many c-Fos positive cells in a given area than their age-matched control group only exposed to the environment for the same amount of time. Significant differences are highlighted in colored and bolded entries, P21 significant differences ($p < 0.05$) = blue and P90 ($p < 0.05$) significant differences = orange, N = 10 and N = 11. S = superficial, I = intermediate and D = deep, M = medial and L = lateral.

(C) Representative coronal sections of one hemisphere from each experimental group with quantified subregions highlighted. +vis = samples from mice with visual stimulation during C-SPOT, Control = mice in arena for 10 min only, no displayed stimuli.

(D) Example of normalized population data obtained from the medial and lateral regions of the superior colliculus from −3.5 AP from P21 mice (blue) versus P90 mice (orange). * = $p < 0.05$, Welch's t-test, followed by Benjamini-Hochberg procedure, N = 10 and 11, P21 versus P90, respectively. Error bars are +/− standard error of the mean.

t-test with correction for multiple comparisons using the Benjamini-Hochberg procedure to decrease the false discovery rate as independence could not be assumed for within subject measures (i.e. AP, ML or depth position) (Figure 4B). This analysis revealed that c-Fos expression is significantly different between P21 and P90 mice in specific subregions of the SC after specific visual experience (Figure 4B, bolded entries). The developmental differences are most prominent along the AP axis. There is an increase in

c-Fos expression related to C-SPOT experience in the anterior region of the SC in juveniles, yet a more significant decrease in c-Fos in the posterior SC of the adults after the C-SPOT experience. The anterior region of the superficial SC corresponds to visual information located within the central/nasal visual field[34] (Figure 4A) and binocular responses are prominent in the anterior SC in the deeper superficial to intermediate layers,[34,35] where specific ipsilateral projections from the retina that are required for optimal prey capture behavior target the SC.[24]

DISCUSSION

Overall, we show significant developmental differences in how mice process stimuli in the binocular visual field during a natural pursuit behavior. It is noteworthy that these behavioral differences correlate with long-known significant differences in binocular visual processing in the mouse visual system at the same age.[1–4]Further, our study finds that the developmental differences in prey pursuit behavior correlates with important developmental differences in cellular activity within the SC where binocular integration occurs.[9] Although it remains unclear how and whether cortical activity differences may contribute to the observed visual stimulus orienting responses, Shank3 knockout mice also fail to execute normal continuous prey pursuits.[37] Shank3 knockout mice are impaired in classical forms of visual cortex plasticity,[27] although SC function and plasticity were not analyzed. It will therefore be important in future work to study the coordinated development of cortical and SC circuits as related to binocular visual processing during this behavior. Indeed, prey capture and the pursuit of "prey-like" visual stimuli, may be ideal behavioral contexts in which to understand the development of corticofugal pathways, spatial orienting behavior and decision-making. In addition, we found a consistent decrease in c-Fos activity during C-SPOT-specific visual experience relative to free exploration in the same environment in the adult. It is unclear why c-Fos levels are reduced in posterior SC and not increased in anterior SC with visual stimulus evoked behavior in adults in this context. It is possible that the increased demands on the juveniles to learn from their experiences to shape binocular function leads to the observed increases of c-Fos in their anterior SC, yet the adults do not have these demands given fully developed binocularity. As both groups of animals were similarly sensitive to responding to stimuli in the peripheral visual field (information that may be reflected in posterior SC), the current study lacks the ability to clearly interpret the reduced posterior c-Fos levels in posterior adult SC during stimulus presentation. As c-Fos expression levels may reflect local responses to growth factors or neuromodulation, or may be localized to other cell types besides neurons,[38] it will be important in future physiological studies of SC activity to compare the anterior- and posterior-most responses over development during this behavior.

Developmental differences in orienting responses to prey and prey-like stimuli were most robust along the nasal to temporal visual field axis. Eye-tracking studies performed in the freely moving adult mouse during prey capture showed that the head angle of the mouse in the azimuth provides an accurate estimate of the position of the binocular visual field.[23,36] Therefore, the evidence in our study argues for more targeted developmental studies of visual stimulus encoding in the regions of SC with binocular responses.[9] However, we did not quantify head pitch and therefore do not provide an estimate of whether developmental biases occur along the upper to lower visual field axis. A previous study of prey capture in mice where the pitch as well as the orientation of the head along the azimuth was quantified found that mice angled their heads downwards during an approach.[23] This would position target stimuli higher up in the relative visual field which is already overrepresented in the topography of the SC relative to the lower visual field.[34] Strikingly, we found few significant differences in c-Fos expression after C-SPOT in either group between the medial (upper visual field) versus lateral (lower visual field) SC. Instead, c-Fos levels increased similarly in both medial and lateral regions of SC only in the juveniles after C-SPOT relative to free exploration. It therefore remains an open question as to whether and how visual information may be processed differently between these two regions of visual space in early development.

An important aspect of this study is demonstrating that C-SPOT can quantify vision in developing mice. This provides a powerful behavioral tool to assess models of neurodevelopmental disorders, Alzheimer's, schizophrenia or other diseases that impact sensory stimulus detection, selection and visual orienting where learning and memory differences could also confound interpretations. Indeed, Autism-associated Shank3 knockout in mice leads to robust deficits in ocular dominance plasticity.[27] It will be interesting to determine whether our assay can more precisely quantify visual perception deficits in these mice and determine how interventions to restore gene and neural circuit function impact vision through development.

Finally, C-SPOT itself is easily modified to screen for a greater diversity of visual features that naturally evoke orienting responses in mice. For example, similar styles of virtual stimulus assays are frequently used to study visual processing and visual system development in the larval zebrafish as related to stimulus size, motion and color.[39,40] Mouse researchers could similarly use C-SPOT to identify visual field biases in processing other visual features not tested in the current study that relate innate behavioral responses to the diversity of receptive field properties so far observed in the visual system of the mouse.[33,41–45]

Limitations of the study

The overall study was designed to discover significant differences in spontaneous visual orienting behavior in P21 mice during natural or naturalistic conditions. However, this work did not assess behavior before P20 and we did not track the eye movements of the mice studied. It therefore remains unknown to what extent eye movement behavior differences measured over finer grained developmental phases explain the observed behavioral deficits in orienting responses of P21 mice. The work reported here also did not test how specific visual experience might change behavior or vision in the developing mice. Finally, c-Fos expression levels, as mentioned previously, provide a limited interpretation of neuronal activity differences between developmental timepoints. More direct measures of neuronal activity in the SC at specific retinotopically mapped positions will be needed in the future to more fully understand how neuronal activity changes during development to support the observed developmental differences in behavior.

STAR★METHODS

Detailed methods are provided in the online version of this paper and include the following:

- KEY RESOURCES TABLE
- RESOURCE AVAILABILITY
  - Lead contact
  - Materials availability
  - Data and code availability
- EXPERIMENTAL MODEL AND SUBJECT DETAILS
- METHOD DETAILS
  - Apparatus
  - Visual stimuli
  - Behavior
  - Immunohistochemistry
- QUANTIFICATION AND STATISTICAL ANALYSIS
  - c-Fos quantification

SUPPLEMENTAL INFORMATION

Supplemental information can be found online at https://doi.org/10.1016/j.isci.2022.105368.

ACKNOWLEDGMENTS

We thank Anastasiya Chevychalova for manually scoring behavior. We greatly appreciate input on drafts of our manuscript from Drs. Jianhua Cang, David Feldheim, Jason Triplett, Angie Michaiel, Philip Parker, Adema Ribic, Katja Reinhard and Karl Farrow.

Funding

This work was supportedby P20GM103650 (J.L.H. and the Cellular and Molecular Imaging core facility), 1R01EY032101 (J.L.H.) and partially supported by NSF grant for an REU site in Biomimetics and Soft Robotics (BioSoRo) with award number EEC grant no. 1852578NSF (J.L.H. and Dr. Yantao Shen).

AUTHOR CONTRIBUTIONS

K.A. collected and analyzed the behavioral and histological data and co-wrote and edited the manuscript. R.G.O. collected and analyzed the live prey capture behavior data. M.K. analyzed histological data. T.F. and S.P. developed the histological approaches used in the manuscript and provided input on experimental design and drafts of the manuscript. J.L.H devised the experiments, coordinated and obtained funding for the study, analyzed the behavioral and histological data, co-wrote and edited the manuscript.

DECLARATION OF INTERESTS

The authors declare no competing interests.

Received: May 31, 2022
Revised: August 4, 2022
Accepted: October 12, 2022
Published: November 18, 2022

REFERENCES

1. Hensch, T.K. (2004). Critical period regulation. Annu. Rev. Neurosci. *27*, 549–579.

2. Cang, J., Savier, E., Barchini, J., and Liu, X. (2018). Visual function, organization, and development of the mouse superior colliculus. Annu. Rev. Vis. Sci. *4*, 239–262.

3. Leighton, A.H., and Lohmann, C. (2016). The wiring of developing sensory circuits-from patterned spontaneous activity to synaptic plasticity mechanisms. Front. Neural Circ. *10*, 71.

4. Hooks, B.M., and Chen, C. (2007). Critical periods in the visual system: changing views for a model of experience-dependent plasticity. Neuron *56*, 312–326.

5. Tan, L., Tring, E., Ringach, D.L., Zipursky, S.L., and Trachtenberg, J.T. (2020). Vision changes the cellular composition of binocular circuitry during the critical period. Neuron *108*, 735–747.e6.

6. Tan, L., Ringach, D.L., and Trachtenberg, J.T. (2022). The development of receptive field tuning properties in mouse binocular primary visual cortex. J. Neurosci. *42*, 3546–3556.

7. May, P.J. (2006). The mammalian superior colliculus: laminar structure and connections. Prog. Brain Res. *151*, 321–378.

8. Ito, S., and Feldheim, D.A. (2018). The mouse superior colliculus: an emerging model for studying circuit formation and function. Front. Neural Circ. *12*, 10.

9. Russell, A.L., Dixon, K.G., and Triplett, J.W. (2022). Diverse modes of binocular interactions in the mouse superior colliculus. J. Neurophysiol. *127*, 913–927.

10. Wheatcroft, T., Saleem, A.B., and Solomon, S.G. (2022). Functional organisation of the mouse superior colliculus. Front. Neural Circ. *16*, 792959.

11. Storchi, R., Rodgers, J., Gracey, M., Martial, F.P., Wynne, J., Ryan, S., Twining, C.J., Cootes, T.F., Killick, R., and Lucas, R.J. (2019). Measuring vision using innate behaviours in mice with intact and impaired retina function. Sci. Rep. *9*, 10396.

12. El-Danaf, R.N., and Huberman, A.D. (2019). Sub-topographic maps for regionally enhanced analysis of visual space in the mouse retina. J. Comp. Neurol. *527*, 259–269.

13. Hoy, J.L., Yavorska, I., Wehr, M., and Niell, C.M. (2016). Vision drives accurate approach behavior during prey capture in laboratory mice. Curr. Biol. *26*, 3046–3052.

14. Dean, P., Redgrave, P., and Westby, G.W. (1989). Event or emergency? Two response systems in the mammalian superior colliculus. Trends Neurosci. *12*, 137–147.

15. Ngo, V., Gorman, J.C., De la Fuente, M.F., Souto, A., Schiel, N., and Miller, C.T. (2022). Active vision during prey-capture in wild marmoset monkeys. Curr. Biol. *32*, 3423–3428.e3. https://doi.org/10.1101/2022.04.01.486794.

16. Klomp, H., and Tinbergen, L. (1960). The natural control of insects in pine woods. Arch. Néerl. Zool. *13*, 344–379.

17. Borghuis, B.G., and Leonardo, A. (2015). The role of motion extrapolation in Amphibian prey capture. J. Neurosci. *35*, 15430–15441.

18. Lin, H.-T., and Leonardo, A. (2017). Heuristic rules underlying dragonfly prey selection and interception. Curr. Biol. *27*, 1124–1137.

19. Roulin, A. (2020). Barn Owls: Evolution and Ecology (Cambridge University Press).

20. Spinka, M., Newberry, R.C., and Bekoff, M. (2001). Mammalian play: training for the unexpected. Q. Rev. Biol. *76*, 141–168.

21. Oldfield, C.S., Grossrubatscher, I., Chávez, M., Hoagland, A., Huth, A.R., Carroll, E.C., Prendergast, A., Qu, T., Gallant, J.L., Wyart, C., and Isacoff, E.Y. (2020). Experience, circuit dynamics, and forebrain recruitment in larval zebrafish prey capture. Elife *9*, e56619. https://doi.org/10.7554/eLife.56619.

22. Procacci, N.M., Allen, K.M., Robb, G.E., Ijekah, R., Lynam, H., and Hoy, J.L. (2020). Context-dependent modulation of natural approach behaviour in mice. Proc. Biol. Sci. *287*, 20201189.

23. Johnson, K.P., Fitzpatrick, M.J., Zhao, L., Wang, B., McCracken, S., Williams, P.R., and Kerschensteiner, D. (2021). Cell-type-specific binocular vision guides predation in mice. Neuron *109*, 1527–1539.e4.

24. Su, J., Sabbagh, U., Liang, Y., Olejníková, L., Dixon, K.G., Russell, A.L., Chen, J., Pan, Y.A., Triplett, J.W., and Fox, M.A. (2021). A cell–ECM mechanism for connecting the ipsilateral eye to the brain. Proc. Natl. Acad. Sci. USA *118*. e2104343118.

25. Hoy, J.L., Bishop, H.I., and Niell, C.M. (2019). Defined cell types in superior colliculus make distinct contributions to prey capture behavior in the mouse. Curr. Biol. *29*, 4130–4138.e5.

26. Igelstrom, K.M., Herbison, A.E., and Hyland, B.I. (2010). Enhanced c-Fos expression in superior colliculus, paraventricular thalamus and septum during learning of cue-reward association. Neuroscience *168*, 706–714.

27. Tatavarty, V., Torrado Pacheco, A., Groves Kuhnle, C., Lin, H., Koundinya, P., Miska, N.J., Hengen, K.B., Wagner, F.F., Van Hooser, S.D., and Turrigiano, G.G. (2020). Autism-associated Shank3 is essential for homeostatic compensation in rodent V1. Neuron *106*, 769–777.e4.

28. Chang, J.T., Whitney, D., and Fitzpatrick, D. (2020). Experience-dependent reorganization drives development of a binocularly unified cortical representation of orientation. Neuron *107*, 338–350.e5.

29. Wang, B.-S., Sarnaik, R., and Cang, J. (2010). Critical period plasticity matches binocular orientation preference in the visual cortex. Neuron *65*, 246–256.

30. Hoffmann, K.P., and Sherman, S.M. (1975). Effects of early binocular deprivation on visual input to cat superior colliculus. J. Neurophysiol. *38*, 1049–1059.

31. Shang, C., Liu, A., Li, D., Xie, Z., Chen, Z., Huang, M., Li, Y., Wang, Y., Shen, W.L., and Cao, P. (2019). A subcortical excitatory circuit for sensory-triggered predatory hunting in mice. Nat. Neurosci. *22*, 909–920.

32. Hoy, J.L., and Niell, C.M. (2015). Layer-specific refinement of visual cortex function after eye opening in the awake mouse. J. Neurosci. *35*, 3370–3383.

33. Basso, M.A., Bickford, M.E., and Cang, J. (2021). Unraveling circuits of visual perception and cognition through the superior colliculus. Neuron *109*, 918–937.

34. Drager, U.C., and Hubel, D.H. (1975). Physiology of visual cells in mouse superior colliculus and correlation with somatosensory and auditory input. Nature *253*, 203–204.

35. Dräger, U.C., and Hubel, D.H. (1976). Topography of visual and somatosensory projections to mouse superior colliculus. J. Neurophysiol. *39*, 91–101.

36. Michaiel, A.M., Abe, E.T., and Niell, C.M. (2020). Dynamics of gaze control during prey capture in freely moving mice. Elife *9*, e57458. https://doi.org/10.7554/eLife.57458.

37. Kuhnle, C.G., Grimes, M., Casanova, V.M.S., Turrigiano, G.G., and Van Hooser, S.D. (2022). Juvenile Shank3 KO mice adopt distinct hunting strategies during prey capture

learning. Preprint at bioRxiv. https://doi.org/10.1101/2022.06.13.495982.

38. Cruz-Mendoza, F., Jauregui-Huerta, F., Aguilar-Delgadillo, A., García-Estrada, J., and Luquin, S. (2022). Immediate early gene c-fos in the brain: focus on glial cells. Brain Sci. *12*, 687.

39. Barker, A.J., and Baier, H. (2015). Sensorimotor decision making in the zebrafish tectum. Curr. Biol. *25*, 2804–2814.

40. Zimmermann, M.J.Y., Nevala, N.E., Yoshimatsu, T., Osorio, D., Nilsson, D.-E., Berens, P., and Baden, T. (2018). Zebrafish differentially process color across visual space to match natural scenes. Curr. Biol. *28*, 2018–2032.e5.

41. Marshel, J.H., Garrett, M.E., Nauhaus, I., and Callaway, E.M. (2011). Functional specialization of seven mouse visual cortical areas. Neuron *72*, 1040–1054.

42. Juavinett, A.L., and Callaway, E.M. (2015). Pattern and component motion responses in mouse visual cortical areas. Curr. Biol. *25*, 1759–1764.

43. Esfahany, K., Siergiej, I., Zhao, Y., and Park, I.M. (2018). Organization of neural population code in mouse visual system. eNeuro *5*. ENEURO.0414, 17.2018. https://doi.org/10.1523/ENEURO.0414-17.2018.

44. Barchini, J., Shi, X., Chen, H., and Cang, J. (2018). Bidirectional encoding of motion contrast in the mouse superior colliculus. Elife *7*, e35261. https://doi.org/10.7554/elife.35261.

45. Lee, K.H., Tran, A., Turan, Z., and Meister, M. (2020). The sifting of visual information in the superior colliculus. Elife *9*, e50678. https://doi.org/10.7554/elife.50678.

46. Gerfen, C.R., Paletzki, R., and Heintz, N. (2013). GENSAT BAC cre-recombinase driver lines to study the functional organization of cerebral cortical and basal ganglia circuits. Neuron *80*, 1368–1383.

47. Mathis, A., Mamidanna, P., Cury, K.M., Abe, T., Murthy, V.N., Mathis, M.W., and Bethge, M. (2018). DeepLabCut: markerless pose estimation of user-defined body parts with deep learning. Nat. Neurosci. *21*, 1281–1289.

48. Aggarwal, M., Zhang, J., Miller, M.I., Sidman, R.L., and Mori, S. (2009). Magnetic resonance imaging and micro-computed tomography combined atlas of developing and adult mouse brains for stereotaxic surgery. Neuroscience *162*, 1339–1350.

49. Wang, Q., and Burkhalter, A. (2013). Stream-related preferences of inputs to the superior colliculus from areas of dorsal and ventral streams of mouse visual cortex. J. Neurosci. *33*, 1696–1705.

STAR★METHODS

KEY RESOURCES TABLE

REAGENT or RESOURCE	SOURCE	IDENTIFIER
Antibodies		
c-Fos	Synaptic Systems	Cat# 226 003, RRID:AB_2231974
DAPI	ThermoFischer Scientific	Cat#62247
Alexa Fluor 488	ThermoFischer Scientific	Cat# A32731, RRID:AB_2633280
Deposited data		
Behaviordata	Mendeley repository	https://doi.org/10.17632/vvxfszxc88.2
c-Fos data	Mendeley repository	https://doi.org/10.17632/ss77yp5nfw.1
Experimental models: Organisms/strains		
Mouse: Ntsr1–GN209–Cre (B6;129S6)	Dr.s Charles Gerfen and Nathanial Heintz	N/A
Mouse: Grp-KH288-Cre (B6;129S6) Dr.s Charles Gerfen and Nathanial Heintz N/A	Dr.s Charles Gerfen and Nathanial Heintz	N/A
C57BL/6J	The Jackson Laboratory	RRID:IMSR_JAX:000664
Software and algorithms		
Custom MATLAB scripts	Mathworks	https://doi.org/10.17632/vvxfszxc88.2
Imaris for Neuroscientists 9.7	BITPLANE-Oxford Instruments	N/A
Psychophysics Toolbox	Dr. David Brainard	N/A
DeepLabCut	Mathis et al., 2018	https://doi.org/10.1038/s41593-018-0209-y

RESOURCE AVAILABILITY

Lead contact

Further information and requests for resources and reagents should be directed to and will be fulfilled by the Lead Contact, Jennifer L. Hoy (Jhoy@unr.edu).

Materials availability

This study did not generate new unique reagents. However, a parts list and tips to create and run the described behavioral assays can be obtained by request from the lead contact.

Data and code availability

- Original c-Fos staining images have been deposited at Mendeley and are publicly available as of the date of publication. The DOI is listed below and in the key resources table. Additional microscopy data reported in this paper will be shared by the lead contact upon request. https://doi.org/10.17632/ss77yp5nfw.1.
- All behavioral data and the original code to analyze the mouse tracks has been deposited at Mendeley and is publicly available as of the date of publication. DOIs are listed below and in the key resources table. https://doi.org/10.17632/vvxfszxc88.2.
- Any additional information required to reanalyze the data reported in this paper is available from the lead contact upon request.

EXPERIMENTAL MODEL AND SUBJECT DETAILS

All mice were used in accordance with protocols approved by the University of Nevada, Reno, Institutional Animal Care and Use Committee, in compliance with the National Institutes of Health Guide for the Care and Use of Laboratory Animals. Both male and female mice were used in the study. We tested 29 P20-22 juvenile mice and 26 adult mice, aged P90 or greater; the specific number used in each statistical comparison is noted in figure legends and results. We used C57BL/6J and mixed background transgenic

mice: Ntsr1-GN209-Cre and Grp-KH288-Cre lines.[46] Mice were group housed, up to 5 animals per cage excluding single housed mice from the study. Mice had *ad libitum* access to water and food (Envigo, Teklad diet, 2919). The vivarium was maintained on a 12 h light/dark schedule, and all behavioral measures were acquired within 3 h of the dark to light transition.

METHOD DETAILS

Apparatus

Mice were individually removed from their home cages and placed into a rectangular, white acrylic open field arena with aluminum slot framing (McMaster-Carr), 60 cm long x 60 cm wide x 30 cm high, with 1/32" thick white buna-N/vinyl rubber flooring (McMaster-Carr) (Figure 2A). A pair of opposing sides of the arena consisted of Hewlett Packard VH240a video monitors that measured 60.5 cm diagonally, with a vertical refresh rate of 50–60 Hz and resolution set to 1920 × 1080 pixels. A solid white background was displayed on both monitors to achieve even lighting throughout the arena. Visual stimuli could then appear on either monitor in C-SPOT trials. Crickets during live prey capture trials were placed into the arena by the experimenter at a location away from the mice. A Logitech HD ProWebcam C920 digital camera was suspended overhead to capture the behavior at 30 frames per second throughout each trial.

Visual stimuli

Visual stimuli for C-SPOT were generated with MATLAB Psychophysics toolbox (Brainard, 1997) and displayed on an LED monitor (60 Hz refresh rate, ~50 cd/m^2 luminance) in a dark room. To mimic insect proportions, we displayed ellipses with a major axis that was 2 times the size of the minor axis. We displayed stimuli that were 2 cm along the horizontal axis as these stimuli evoked the most frequent approaches in adult mice and more approaches to this stimulus were specifically increased after live prey capture experience in the adult.[22] A 2 cm long stimulus corresponds to a relative stimulus size of ~4° from 30 cm away from the screen. Stimulus speed was kept constant at 2 cm/s as this speed evoked the most approach and least amount of arrests in adult mice.[22] Stimuli were on the screen for 30 s before disappearing for 7 s and then reappearing. This pattern repeated throughout the overall trial, 300 s.

Behavior

Mice were acclimated to handlers and arena for 4 days prior to either the live prey capture assay or virtual task. During habituation, mice were handled 3 times a day for 3 min each and placed in the arena 3 times a day for 5 min each time. Young mice were habituated to handler and environment 3–4 days prior to their tested age of P20-22. On the testing/behavioral measurement day, group housed mice were brought into the testing room in their home cages and allowed to acclimate to the darkened testing room. Then, each experimental subject was placed in the testing arena and habituated for 3–5 min, with controlled illumination emitted from computer screen monitors only. Either C-SPOT was run, or live crickets were introduced and behavior recorded, but all mice were naive to other testing conditions in order to assess innate responses. The arena was cleaned with 70% EtOH after each mouse was removed to mitigate odor distractions. Exposing mice to stimuli did not begin until each mouse demonstrated self-grooming behaviors and reduced defecation and thigmotaxic behavior which were taken as indications they were not anxious in the environment, again, around 3–5 min.

For testing prey capture behavior, mice were given 10 min with the cricket after habituation and were not food deprived in order to understand how visual stimuli were interpreted at an individual's baseline state. This study only quantified the first day of behavior in response to live crickets in order to quantify naive/innate responses. All mice were then returned to their home cages with standard food. The crickets used were *Acheta domestica* obtained from Fluker's Farm or a local pet store and were 1–2 cm in length, group-housed, and fed Fluker's Orange Cube Cricket Diet.

DeepLabCut[47] was used to digitize and extract 2-dimensional coordinates of the mouse's nose, two ears and body center, as well as the center point of the stimulus (cricket or computer-generated stimulus) throughout the video recordings at 30Hz. These tracks were entered into customized MATLAB scripts to extract behavioral parameters: mouse speed, stimulus speed, stimulus angle, range, subjective stimulus size and speed.

An arrest "response" was defined as any time the mouse's nose and body moved less than 0.5 cm/s for a duration of 0.5–2 s. Arrests that occurred in the absence of a visual stimulus, or when the stimulus was more than 140° from the bearing of the nose, were excluded from analysis of visual driven arrest responses. Approach starts were defined as mice moving toward the stimulus starting from a distance of at least 8 cm, and at an average approach speed of at least 15 cm/s and a stimulus bearing of less than 150°. Using these definitions, we computed the percentage of stimulus trials in which each behavior was observed, as well as the number of arrests and approaches that occurred during individual trials. A successful approach was defined as any time the mouse's nose came within 3 cm of the stimulus after an approach start had been identified.

For both response types, approach or arrest, we calculated range as the distance between the center of the head between the two ears and the center of the stimulus, and stimulus angle as the angular distance between the line emanating from the center of the mouse body to the mouse nose, and that from the center of the mouse body to the center of the stimulus. Angular stimulus sizes and speeds were calculated using the horizontal length of the stimulus (2 cm) and the distance of the behavioral event from the stimulus in cm.

Immunohistochemistry

To assay c-Fos expression in mice exposed to C-SPOT and age-matched controls without visual stimulation and experience, mice were deeply anesthetized 90 min after behavioral testing through inhalation with 3.5% isoflurane. Subjects were then transcardially perfused with 75 mL of phosphate buffered saline (1X PBS) followed with 25 mL of 4% paraformaldehyde (PFA). Brains were removed and stored in 4% PFA for 24 h at 4°C.

Brains were then removed from PFA and rinsed with PBS before sectioning into 45 μm thick coronal sections. Floating sections were stored in 0.02% sodium azide (NaN_3) and PBS at 4°C for up to two weeks before assaying for c-Fos protein expression. To assay c-Fos protein expression, floating sections in well dishes were incubated in a blocking solution (4% bovine serum albumin (BSA), 2% horse serum, 0.2% Triton X-100, 0.05% NaN_3) for 3 h, followed by incubation with rabbit anti-c-Fos primary antibody (1:500, 226 003, Synaptic Systems) in blocking solution for 24 h at 4°C. Sections were washed 3 times for 20 min each time in PBS at 20°C before incubating with goat anti-rabbit Alexa 488 secondary antibody (1:500, A32723 Invitrogen) in blocking solution for 2 h at 20°C. Sections were then incubated in DAPI (1:1000, 64427, ThermoFischer Scientific; 15 min at 20°C) diluted in PBS for nuclei labeling. Sections were washed again 3 times for 20 min each time before mounting onto slides with AquaPoly mounting media (18,606, Polysciences). Mounted sections were stored at 4°C in dark slide boxes until image processing.

QUANTIFICATION AND STATISTICAL ANALYSIS

Statistics on behavioral measures were performed using MATLAB and R software. Where means are reported and data are normally distributed we used Welch's t-test (two group comparisons), followed by Benjamini-Hochberg procedure to decrease false discovery rate and correct for multiple comparisons. The specific tests used are specified in figure legends. Where medians are reported and/or data are not normal, rank sum tests were used. Significant differences in proportional measures were determined by Fisher exact test. Test results with a p value of <0.05 were considered significant. Cohen's $D > 0.8$ considered a large effect, with all significant effects in this study having Cohen's $D > 0.8$. All sample sizes, statistical tests used and central tendency values and measures of dispersion and precision are reported in corresponding figure legends. This information for data not represented in the figures is reported in the results where relevant.

c-Fos quantification

Images were obtained using a Leica Confocal microscope. Tile scans of the entirety of each coronal slice was imaged with a 20X objective and saved as a LIF image file. Sections between −3.5 and −4.6 AP were imaged. Specific regions and structures in the adult were identified as in Paxinos and Franklin's the Mouse Brain in Stereotaxic Coordinates and the Allen Mouse Brain Coronal Atlas (https://mouse.brain-map.org/static/atlas). Developmentally similar regions were confirmed using a magnetic resonance imaging and micro-computed tomography combined atlas of developing mouse brains.[48] Subregions and laminae of colliculus were identified as in Wang and Burkhalter, 2013.[49]

c-Fos positive cells were identified and quantified using Imaris Microscopy Image Analysis Software (Oxford Instruments). LIF files were loaded into IMARIS and Gamma correction (0.8%) and background subtraction were standardized and applied similarly to all images. Images were analyzed blind to testing condition. Three circular regions of interest (ROIs) were drawn in each collicular layer: superficial, intermediate, and deep in both the medial and lateral regions. To ensure similarity of subregions quantified between subjects, ROIs for the medial region spanned the center of a region as measured from the brain's midline (medial border) to the medial/lateral border of the section (halfway to 2/3 between the medial-lateral borders of the SC, Figure 4C). Lateral ROIs were drawn halfway from the medial/lateral border of the section to the lateral border of the SC. The number of c-Fos positive cells and DAPI positive cells for each ROI were used to create a ratio of c-Fos:DAPI fluorescence. These percentages were then averaged per medial or lateral region, and again averaged between 2–3 sections for each AP region for each subject. These "per subject" percent averages were then used to determine the relative increase in c-Fos positive cells between visually-stimulated mice and their controls (age-matched and exposed to environment only). The reported normalized metric "ratio of c-Fos expression (w to w/o)" is each experimental subject's percent of c-Fos positive cells divided by the average percentage obtained from their age-matched controls that were placed in the same environment with no visual stimulation. This therefore compares the percent increase in c-Fos positive cells when mice view and respond to visual stimuli in our testing arena, versus when mice wander in the same arena without the specific visual experience assayed.